ChemComm

COMMUNICATION

View Article Online
View Journal | View Issue

Cite this: *Chem. Commun.*, 2023, **59**, 1094

Received 29th October 2022,
Accepted 16th December 2022

DOI: 10.1039/d2cc05879k

rsc.li/chemcomm

Targeted photothermal release of antibiotics by a graphene nanoribbon-based supramolecular glycomaterial†

Ying Shang,‡[a] Sheng Zhang,‡[a] Hui-Qi Gan,‡[a] Kai-Cheng Yan,[ae] Fugui Xu,[b] Yiyong Mai,[b] Daijie Chen,[c] Xi-Le Hu,*[a] Lei Zou,*[a] Tony D. James*[ef] and Xiao-Peng He*[ad]

Here, we report the simple construction of a supramolecular glycomaterial for the targeted delivery of antibiotics to *P. aeruginosa* in a photothermally-controlled manner. A galactose-pyrene conjugate (Gal-pyr) was developed to self-assemble with graphene nanoribbon-based nanowires *via* π–π stacking to produce a supramolecular glycomaterial, which exhibits a 1250-fold enhanced binding avidity toward a galactose-selective lectin when compared to Gal-pyr. The as-prepared glycomaterial when loaded with an antibiotic that acts as an inhibitor of the bacterial folic acid biosynthetic pathway eradicated *P. aeruginosa*-derived biofilms under near-infrared light irradiation due to the strong photothermal effect of the nanowires accelerating antibiotic release.

Bacterial infection is a global public health problem that results in nearly five million deaths annually.[1] With the overuse of antibiotics, a number of multidrug-resistant bacteria have emerged, which poses significant challenges to clinicians as well as to the pharmaceutical industry.[2] Consequently, numerous and elegant systems based on a variety of organic and inorganic materials have been developed for the enhanced delivery of antibiotics to bacterial cells.[3] Moreover, smart delivery systems for stimulus-responsive release of antibiotics based on metal-organic frameworks, hydrogels, organic polymers and inorganic nanoparticles, which could be selectively activated by specific microenvironmental factors (*e.g.*, pH, thiols, ROSs) at the infection site, have also been recently developed.[4]

To enhance the precision with which antibiotics are delivered to bacteria, antibody-antibiotic conjugates (AACs) have been developed.[5] However, the expression and purification of antibodies are labor-extensive and expensive, and the covalent coupling between antibodies and small-molecule antibiotics is generally low in yield. Therefore, the development of alternative strategies to achieve targeted antibiotic delivery remains an unmet need.

Selective sugar-protein interactions are implicated in several important biological processes.[6] Bacteria are known to express functional sugar-recognition proteins (or lectins). For example, the adhesive protein, FimH expressed by the uro-pathogenic *Escherichia coli* (UPEC), facilitates bacterial adhesion to urinary epithelium through selective recognition of the mannosyl residues on the surface of epithelial cells.[7] Soluble lectins, Lec A and Lec B, expressed by *Pseudomonas aeruginosa* (*P. aeruginosa*) selectively bind to galactose and fucose, respectively, facilitating the adhesion of *P. aeruginosa* to endothelial cells.[8] By targeting bacterial lectins, a variety of glycoclusters and glycopolymers have been synthesized for blocking bacterial adhesion to host cells.[9]

Here, we report a simple strategy for the construction of supramolecular glycomaterials capable of the targeted delivery of antibiotics to *P. aeruginosa* that express Lec A and Lec B. We synthesized a pyrene-modified galactoside that targets Lec A of *P. aeruginosa*. Since multivalency is important for monosaccharides to achieve high-avidity binding with lectins, we used

[a] *Key Laboratory for Advanced Materials and Joint International Research Laboratory of Precision Chemistry and Molecular Engineering, Feringa Nobel Prize Scientist Joint Research Center, School of Chemistry and Molecular Engineering, East China University of Science and Technology, 130 Meilong Rd., Shanghai 200237, China. E-mail: xphe@ecust.edu.cn, zoulei@ecust.edu.cn, xlhu@ecust.edu.cn*

[b] *School of Chemistry and Chemical Engineering, Frontiers Science Center for Transformative Molecules, Shanghai Key Laboratory of Electrical Insulation and Thermal Ageing, Shanghai Jiao Tong University, 800 Dongchuan RD. Minhang District, Shanghai 200240, China*

[c] *School of Pharmacy, Shanghai Jiao Tong University, 800 Dongchuan RD. Minhang District, Shanghai 200240, China*

[d] *National Center for Liver Cancer, the International Cooperation Laboratory on Signal Transduction, Eastern Hepatobiliary Surgery Hospital, Shanghai 200438, China*

[e] *Department of Chemistry, University of Bath, Bath, BA2 7AY, UK. E-mail: t.d.james@bath.ac.uk*

[f] *School of Chemistry and Chemical Engineering, Henan Normal University, Xinxiang 453007, China*

† Electronic supplementary information (ESI) available: Experimental section, additional figures and original spectral copies of new compounds. See DOI: https://doi.org/10.1039/d2cc05879k

‡ Equal contribution.

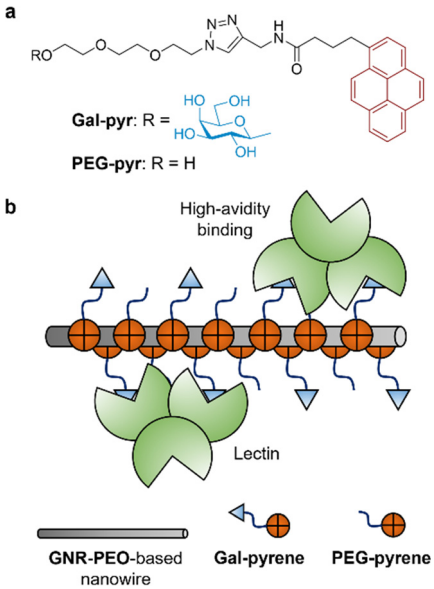

Fig. 1 (a) Structure of galactosyl pyrene (**Gal-pyr**) and poly(ethyleneglycol) (PEG)-modified pyrene (**PEG-pyr**). (b) Schematic illustration of the supramolecular glycomaterial formed between **Gal-pyr**, **PEG-pyr** and a graphene nanoribbon (**GNR-PEO**)-based nanowire for high-avidity binding with oligomeric lectins.

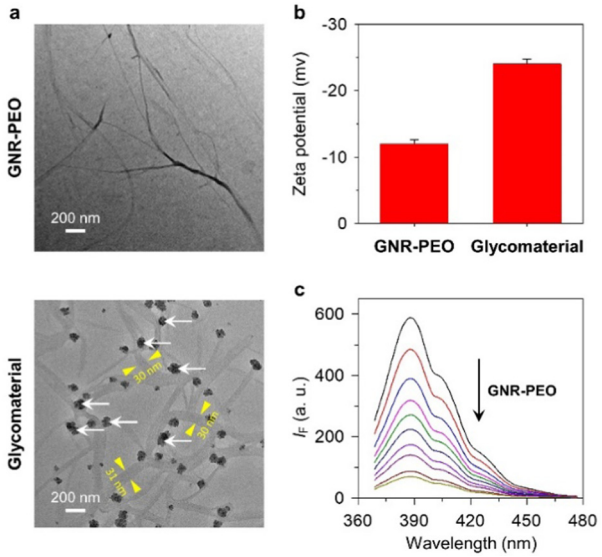

Fig. 2 (a) Transmission electron microscopic images of **GNR-PEO** (7.5 μg mL^{-1}) and the supramolecular glycomaterial (**PEG-pyr/Gal-pyr/GNR-PEO** = 3 μM/7 μM/7.5 μg mL^{-1}); the white arrows indicate the **Gal-pyr/PEO-pyr** aggregates assembled onto the surface of **GNR-PEO**-based nanowires, and the yellow arrows measure the widths of nanowires. (b) Zeta potential of **GNR-PEO** (7.5 μg mL^{-1}) and the supramolecular glycomaterial (**PEG-pyr/Gal-pyr/GNR-PEO** = 3 μM/7 μM/7.5 μg mL^{-1}) in deionized water. (c) Fluorescence spectra of **Gal-pyr** (7 μM) with increasing concentrations of **GNR-PEO** (0–12 μg mL^{-1}) in deionized water (excitation wavelength = 370 nm).

graphene nanoribbon-based nanowires whose photothermal conversion efficiency has proven to be higher than those of several popular low-dimensional materials including gold nanoparticles, single-walled carbon nanotubes, graphene oxide and thin-layer molybdenum disulfide as a backbone to cluster the pyrenyl galactosides (Fig. 1).[10] The glycomaterial could load a variety of different antibiotics and exhibited near-infrared (NIR) light-activated release of the antibiotics to *P. aeruginosa* facilitated by sugar-lectin recognition.

The pyrene-modified galactoside (**Gal-pyr**) was synthesized using the Cu(I)-catalyzed azide–alkyne 1,3-dipolar cycloaddition (CuAAC) click reaction between an azido β-*O*-galactoside and *N*-propynyl pyrene in 82% yield (Scheme S1, ESI†). **PEG-pyr** without the galactosyl group was synthesized as a control (Scheme S1, ESI†). Then, **Gal-pyr** and/or **PEG-pyr** was self-assembled with the nanowires formed from the previously synthesized water soluble **GNR-PEO** *via* π–π stacking,[11] generating supramolecular glycomaterials (**PEG-pyr/Gal-pyr/GNR-PEO**).

We used transmission electron microscopy (TEM) for morphological characterization. From representative TEM images, we observed wire-like microstructures for the **GNR-PEO**-based nanowires (Fig. 2a),[12] and particle-like species corresponding to **PEG-pyr** and **Gal-pyr** aggregates were seen on the surface of the nanowires for **PEG-pyr/Gal-pyr/GNR-PEO** (Fig. 2b). The absolute zeta potential for **PEG-pyr/Gal-pyr/GNR-PEO** was larger than that of the **GNR-PEO**-based nanowire when dispersed in deionized water (Fig. 2c) as determined by dynamic light scattering. This suggests that the presence of the pyrenyl galactosides enhances the aqueous stability of the nanowires.[13] Increasing concentrations of **GNR-PEO**-based nanowires added to deionized water solutions of **Gal-pyr** gradually quenched the fluorescence of the latter (Fig. 2d), which is probably due to the Förster resonance energy transfer from pyrene to the **GNR-PEO** after self-assembly.[14] Moreover, the amount of **PEG-pyr** and **Gal-pyr** on the nanowires was quantified using the anthrone method (Fig. S1, ESI†) and thermal gravimetric analysis (Fig. S2, ESI†).

Next, we measured the binding strength between the supramolecular glycomaterials and peanut agglutinin (PNA), a plant lectin known to selectively recognize galactose. A well-established fluorescence titration assay[15] was used to determine the binding constant (K_a) between the materials and PNA (Fig. S3 and S4, ESI†). Since the regular distribution of glycosyl groups on a material backbone is crucial for lectin binding,[16] we prepared a series of supramolecular glycomaterials containing both **PEG-pyr** and **Gal-pyr** with **GNR-PEO** at different molar ratios. We envisioned that the co-existence of **PEG-pyr** on the surface of **GNR-PEO** would disperse the **Gal-pyr** molecules thereby facilitating a more effective binding with the oligomeric lectins. Indeed, using a fluorescence titration assay, we determined that the binding constant (K_a) of the glycomaterials differs as the molar ratio of **PEG-pyr** and **Gal-pyr** changes. A **PEG-pyr/Gal-pyr** ratio of 3 : 7 resulted in the strongest binding with PNA ($K_a = 1.1 \times 10^8$ M^{-1}) and increasing the ratio from 4 : 6 to 9 : 1 resulted in a decrease of the K_a (Table S1, ESI†). Significantly, the K_a of **GNR-PEO** with a **PEG-pyr/Gal-pyr** ratio of 3 : 7 was *ca.* 1250-fold stronger than that of just **Gal-pyr** ($K_a = 0.009 \times 10^7$ M^{-1}), confirming that our supramolecular strategy enhances the binding avidity of the glycomaterial with

PNA. A thorough comparison to previously developed glycoclusters and glycopolymers suggests that our supramolecular glycomaterial is among the strongest in terms of PNA binding (Table S2, ESI†). To prove that the binding is dependent on galactose-PNA recognition, we pre-treated PNA with an excess of free β-D-galactose (Gal) (10 mM). This resulted in an 18000-fold decrease in binding constant ($K_a = 6.2 \times 10^3\ M^{-1}$) between the glycomaterial and PNA (Fig. S5, ESI†).

Trimethoprim (**TMP**) is a commercial antibiotic that inhibits dihydrofolate reductase (DHFR) conserved in bacterial species, resulting in bacterial death due to a lack of folic acid.[17] To prepare the antibiotic-loaded system (**TMP/PEG-pyr/Gal-pyr/GNR-PEO**), **TMP** was added to a deionized water solution of **PEG-pyr/Gal-pyr/GNR-PEO**, followed by sonication (100 W) for 60 min. The loading efficiency of **PEG-pyr/Gal-pyr/GNR-PEO** for **TMP** was determined to be 69.7% with a loading of 691 μg mL^{-1} (Fig. S6a, ESI†). We then evaluated whether the photothermal properties of the **GNR-PEO** nanowire could facilitate the release of **TMP** from the glycomaterial. A deionized water solution of **TMP/PEG-pyr/Gal-pyr/GNR-PEO** was irradiated with 808 nm laser for 0–12 h, centrifuged, and then the supernatants were collected and analyzed using UV-vis spectroscopy to monitor **TMP** release. A minimal amount of **TMP** was detected in the supernatants in the absence of light irradiation over 12 h (Fig. S6b, ESI†), however, when light irradiation was applied the antibiotic was released from the glycomaterial system at a rate of 29.2 μg mL^{-1} per hour (Fig. S6c, ESI†). This suggests that the heat generated *in situ* by **GNR-PEO**-based nanowires upon NIR light irradiation enables a photothermally-controlled release of the antibiotic.[18]

Next, we evaluated the antibacterial activities of the supramolecular glycomaterial. **TMP/GNR-PEO** without and with a **PEG-pyr/Gal-pyr** ratio of 3 : 7 was incubated with *P. aeruginosa* (ATCC 27853) for 3 h without (−) or with (+) 808 nm light irradiation. **TMP**, **TMP/PEG-pyr/Gal-pyr** (3 : 7) and **TMP/GNR-PEO** were used as control. We first determined that **TMP/GNR-PEO** without **PEG-pyr/Gal-pyr** loading was slightly toxic to *P. aeruginosa* in the absence (59.8% viability) and presence (44.2% viability) of light irradiation. The bacterial viability of the **TMP/PEG-pyr/Gal-pyr/GNR-PEO** group was found to be 50.3%. This value further decreased to 22.4% when light irradiation was applied, which is significantly lower than those of **TMP** (60.9%) and mixtures of **TMP** and **PEG-pyr/Gal-pyr** (3 : 7) (61.6%) groups (Fig. 3a). These results suggest that the supramolecular glycomaterial facilitates the delivery of **TMP** to *P. aeruginosa* cells in a photothermally-driven manner. A competition assay by pre-treatment with free D-galactose of the *P. aeruginosa* reduced the activity of the glycomaterial by 22.5% (Fig. S7, ESI†). This suggests that the antibacterial activity of **TMP/PEG-pyr/Gal-pyr/GNR-PEO** is dependent on galactose-Lec A recognition.

The generality of the glycomaterial system was examined using two additional antibiotics, levofloxacin (**Lev**) and cefoperazone-sulbactam (**Cef-sul**). We determined that the **Lev/PEG-pyr/Gal-pyr/GNR-PEO** and **Cef-sul/PEG-pyr/Gal-pyr/GNR-PEO** material with 808 nm light irradiation exhibited a 1.85-fold and 1.70-fold improved antibacterial activity than **Lev** (Fig. 3b) and **Cef-sul** (Fig. 3c) alone, respectively. This suggests that the glycomaterial is generally suitable for targeted delivery of structurally different antibiotics.

Finally, the supramolecular glycomaterial was used to eradicate biofilms formed by *P. aeruginosa*. We determined that the addition of just **TMP** or **PEG-pyr/Gal-pyr/GNR-PEO** to the biofilm induced 31% and 24% bacterial death, as well as a decrease in CFU (colon-forming units) count to $10^{3.9}$ cells per mL and $10^{4.3}$ cells per mL, respectively (Fig. 4). The use of **TMP/PEG-pyr/Gal-pyr/GNR-PEO** without light caused a moderate level of bacterial death (51% dead bacteria) and a decrease in CFU count to 10^2 cells per mL, which suggests that the antibiotic was slowly released in the complicated environment of the biofilm. Notably, while no substantial changes in antibacterial effect were observed for **TMP** or **PEG-pyr/Gal-pyr/GNR-PEO** under NIR light irradiation, the use of light enhanced the activity of **TMP/PEG-pyr/Gal-pyr/GNR-PEO** to eradicate the biofilm (74% dead bacteria detected) and caused a decrease in CFU count to $10^{1.5}$ cells per mL. The results from the staining method agrees

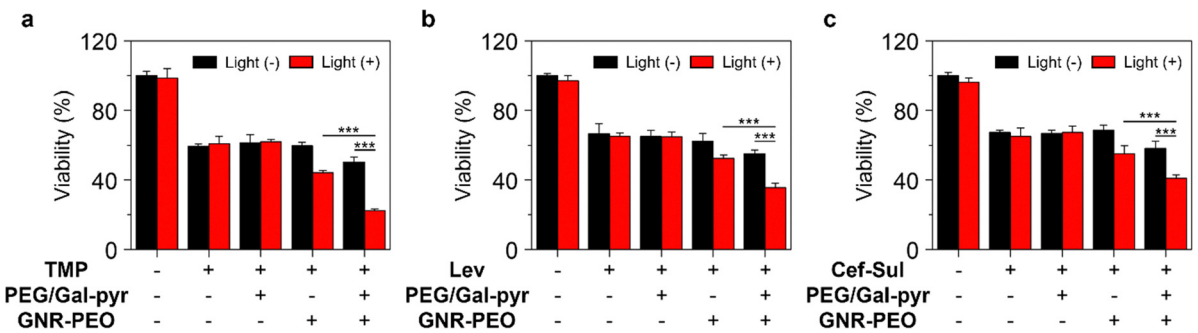

Fig. 3 Viability of *P. aeruginosa* (ATCC 27853) in the absence and presence of (a) **TMP** (150 μg mL^{-1}), **TMP/PEG-pyr/Gal-pyr** (150 μg mL^{-1}/6 μM/14 μM), **TMP/GNR-PEO** (150 μg mL^{-1}/15 μg mL^{-1}) and **TMP/PEG-pyr/Gal-pyr/GNR-PEO** (150 μg mL^{-1}/6 μM/14 μM/15 μg mL^{-1}), (b) **Lev** (0.25 μg mL^{-1}), **Lev/PEG-pyr/Gal-pyr** (0.25 μg mL^{-1}/6 μM/14 μM), **Lev/GNR-PEO** (0.25 μg mL^{-1}/15 μg mL^{-1}) and **Lev/PEG-pyr/Gal-pyr/GNR-PEO** (0.25 μg mL^{-1}/6 μM/14 μM/15 μg mL^{-1}), and (c) **Cef-Sul** (2 μg mL^{-1}), **Cef-Sul/PEG-pyr/Gal-pyr** (2 μg mL^{-1}/6 μM/14 μM), **Cef-Sul/GNR-PEO** (2 μg mL^{-1}/15 μg mL^{-1}) and **Cef-Sul/PEG-pyr/Gal-pyr/GNR-PEO** (2 μg mL^{-1}/6 μM/14 μM/15 μg mL^{-1}) with and without NIR light irradiation (808 nm, 1 W cm^{-2}, 15 min). Error bars mean standard deviation (n = 3); ***$P < 0.001$.

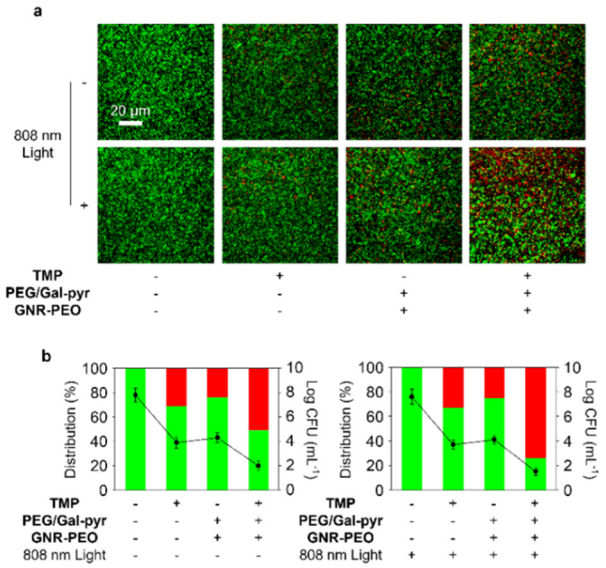

Fig. 4 Fluorescence imaging (a) and quantification (b) of the live and dead bacterial cells in *P. aeruginosa* (ATCC 27853)-based biofilms in the absence and presence of **TMP** (150 μg mL^{-1}), **PEG-pyr/Gal-pyr/GNR-PEO** (6 μM/14 μM/15 μg mL^{-1}) and **TMP/PEG-pyr/Gal-pyr/GNR-PEO** (150 μg mL^{-1}/6 μM/14 μM/15 μg mL^{-1}) without and with light irradiation (808 nm, 1 W cm^{-2}, 15 min). Error bars mean standard deviation (n = 3).

well with those from the counting method, confirming that the system is applicable for the photothermally-controlled release of antibiotics in bacterial biofilms.

In summary, we developed a supramolecular glycomaterial, in which the multivalent exposure of pyrenyl galactose on the surface of **GNR-PEO**-based nanowire resulted in high binding avidity with PNA. The glycomaterial achieved the targeted release of antibiotics to *P. aeruginosa* in a photothermally-controlled fashion. This led to the effective eradication of biofilms formed by *P. aeruginosa*. This research provides new insight into the development of supramolecular glycomaterials for the targeted, photocontrolled release of antibiotics for the effective treatment of bacterial infections.

The authors thank the Natural National Science Foundation of China (NSFC) (No. 91853201, 21907030, 82130099 and 52203268), the Fundamental Research Funds for the Central Universities (222201717003), the Programme of Introducing Talents of Discipline to Universities (B16017) and Open Funding Project of the State Key Laboratory of Bioreactor Engineering of East China University of Science and Technology for financial support. The Research Center of Analysis and Test of East China University of Science and Technology is gratefully acknowledged for assistance in analytical experiments. TDJ wishes to thank the Royal Society for a Wolfson Research Merit Award and the Open Research Fund of the School of Chemistry and Chemical Engineering, Henan Normal University for support (2020ZD01).

Conflicts of interest

The authors have no conflict of interest to declare.

Notes and references

1 C. J.-L. Murray, K.-S. Ikuta, F. Sharara, L. Swetschinski, G.-R. Aguilar and A. Gray, *Lancet*, 2022, **399**, 629–655.
2 (*a*) M. A. Farha and E. D. Brown, *Nat. Microbiol.*, 2019, **4**, 565–577; (*b*) U. Theuretzbacher, K. Outterson, A. Engel and A. Karlen, *Nat. Rev. Microbiol.*, 2020, **18**, 275–285.
3 P. C. Ray, S. A. Khan, A. K. Singh, D. Senapati and Z. Fan, *Chem. Soc. Rev.*, 2012, **41**, 3193–3209.
4 (*a*) D. F. Sava Gallis, K. S. Butler, J. O. Agola, C. J. Pearce and A. A. McBride, *ACS Appl. Mater. Interfaces*, 2019, **11**, 7782–7791; (*b*) H. M. Ren, L. Hua, L. J. Zhang, Y. Q. Zhao, C. Y. Lei and Z. P. Xiu, *Nano Today*, 2022, **44**, 101489; (*c*) Y. Wang, Q. Yuan, W. Feng, W. Pu, J. Ding and H. Zhang, *J. Nanobiotechnol.*, 2019, **17**, 103–118; (*d*) D. Alkekhia, C. LaRose and A. Shukla, *ACS Appl. Mater. Interfaces*, 2022, **14**, 27538–27550.
5 (*a*) S. Lehar, T. Pillow, M. Xu, L. Staben, K. Kajihara and R. Vandlen, *Nature*, 2015, **527**, 323–328; (*b*) S. Mariathasan and M. W. Tan, *Trends Mol. Med.*, 2017, **23**, 135–149.
6 J. Poole, C. J. Day, M. von Itzstein, J. C. Paton and M. P. Jennings, *Nat. Rev. Microbiol.*, 2018, **16**, 440–452.
7 N. M. Poole, S. I. Green, A. Rajan, L. E. Vela, X. L. Zeng and M. K. Estes, *Infect. Immun.*, 2017, **85**, e00581–17.
8 C. Chemani, A. Imberty, S. de Bentzmann, M. Pierre, M. Wimmerová and B. P. Guery, *Infect. Immun.*, 2009, **77**, 2065–2075.
9 (*a*) A. Bernardi, J. Jimenez-Barbero, A. Casnati, C. De Castro, T. Darbre, F. Fieschi, J. Finne, H. Funken, K. E. Jaeger, M. Lahmann, T. K. Lindhorst, M. Marradi, P. Messner, A. Molinaro, P. V. Murphy, C. Nativi, S. Oscarson, S. Penades, F. Peri, R. J. Pieters, O. Renaudet, J. L. Reymond, B. Richichi, J. Rojo, F. Sansone, C. Schaffer, W. B. Turnbull, T. Velasco-Torrijos, S. Vidal, S. Vincent, T. Wennekes, H. Zuilhof and A. Imberty, *Chem. Soc. Rev.*, 2013, **42**, 4709–4727; (*b*) S. Cecioni, A. Imberty and S. Vidal, *Chem. Rev.*, 2015, **115**, 525–561.
10 (*a*) Y. Huang, W.-T. Dou, F. Xu, H.-B. Ru, Q. Gong, D. Wu, D. Yan, H. Tian, X.-P. He, Y. Mai and X. Feng, *Angew. Chem., Int. Ed.*, 2018, **57**, 3366–3371; (*b*) X.-L. Hu, L. Chu, X. Dong, G.-R. Chen, T. Tang, D. Chen, X.-P. He and H. Tian, *Adv. Funct. Mater.*, 2019, **29**, 1806986; (*c*) X.-L. Hu, N. Kwon, K.-C. Yan, A. C. Sedgwick, G.-R. Chen, X.-P. He, T. D. James and J. Yoon, *Adv. Funct. Mater.*, 2020, **30**, 1907906; (*d*) C. Zhang, D.-T. Shi, K.-C. Yan, A. C. Sedgwick, G.-R. Chen, X.-P. He, T. D. James, B. Ye, X.-L. Hu and D. Chen, *Nanoscale*, 2020, **12**, 23234–23240.
11 K. Zhang, Y. X. Hu, L. Z. Wang, M. J. Monteiro and Z. F. Jia, *ACS Appl. Mater. Interfaces*, 2017, **9**, 34900–34908.
12 Z.-H. Yu, X. Li, F. Xu, X.-L. Hu, J. Yan, N. Kwon, G.-R. Chen, T. Tang, X. Dong, Y. Mai, D. Chen, J. Yoon, X.-P. He and H. Tian, *Angew. Chem., Int. Ed.*, 2020, **59**, 3658–3664.
13 N. J. Silva, I. Borges Jr, P. A. Tone, M. J. Green, H. Lischka and A. J. A. Aquino, *Chem. Phys.*, 2019, **527**, 110468.
14 (*a*) S. Osella, M. Kiliszek, E. Harputlu, C. G. Unlu, K. Ocakoglu, J. Kargul and B. Trzaskowski, *J. Mater. Chem. C*, 2018, **6**, 5046–5054; (*b*) W.-T. Dou, X. Wang, T. Liu, S. Zhao, J.-J. Liu, Y. Yan, J. Li, C.-Y. Zhang, A. C. Sedgwick, H. Tian, J. L. Sessler, D.-M. Zhou and X.-P. He, *Chemistry*, 2022, **6**, 1750–1761; (*c*) W.-T. Dou, H.-H. Han, A. C. Sedgwick, G.-B. Zhu, Y. Zang, X.-R. Yang, J. Yoon, T. D. James, J. Li and X.-P. He, *Sci. Bull.*, 2022, **67**, 853–878.
15 K. Hatano, H. Saeki, H. Saeki, H. Aizawa, T. Koyama and K. Koyama, *Tetrahedron Lett.*, 2009, **50**, 5816–5819.
16 A. Battigelli, J. H. Kim, D. C. Dehigaspitiya, C. Proulx, E. J. Robertson, D. J. Murray, B. Rad, K. Kirshenbaum and R. N. Zuckermann, *ACS Nano*, 2018, **12**, 2455–2465.
17 (*a*) S. M. Reeve, D. Si, J. Krucinska, Y. Yan, K. Viswanathan, S. Wang, G. T. Holt, M. S. Frenkel, A. A. Ojewole, A. Estrada, S. S. Agabiti, J. B. Alverson, N. D. Gibson, N. D. Priestley, A. J. Wiemer, B. R. Donald and D. L. Wright, *ACS Infect. Dis.*, 2019, **5**, 1896–1906; (*b*) C.-J. Zhong, X.-L. Hu, X.-L. Yang, H.-Q. Gan, K.-C. Yan, F.-T. Shu, P. Wei, T. Gong, P.-F. Luo, T. D. James, Z.-H. Chen, Y.-J. Zheng, X.-P. He and Z.-F. Xia, *ACS Appl. Mater. Interfaces*, 2022, **14**, 39808–39818.
18 N. S. H. Motlagh, P. Parvin, Z. H. Mirzaie, R. Karimi, J. H. Sanderson and F. Atyabi, *Biomed. Opt. Express*, 2020, **11**, 3783–3794.